QUANTUM-CHEMICAL MO STUDY OF PROTONATION OF 1-METHYL-1,4-DIHYDRONICOTINAMIDE*

Jiří KRECHL, Stanislav BÖHM and Josef KUTHAN

Department of Organic Chemistry,
Prague Institute of Chemical Technology, 166 28 Prague 6

Received October 15th, 1981

The methods EHT, CNDO/2, MNDO and *ab initio* STO-3G have been used to study regioselectivity of protonation of 1-methyl-1,4-dihydronicotinamide (*I*, R = CH_3). The results obtained are discussed in relation to lability of the NAD(P)H coenzymes in acid media and agree well with experimental findings.

Reduction of some substrates by action of NAD(P)H and its models seems to involve an inevitable prelude – acid catalysis[1-4] activating *e.g.* carbonyl compounds as it follows:

$$R^1R^2CO + AH^{(+)} \rightleftharpoons R^1R^2C^{(+)}OH + A$$

In an enzymatic reduction the role of $AH^{(+)}$ cofactor can *e.g.* be played by the protonated form of imidazole ring of histidine near active centre of the apoenzyme[3,5,6]. It was observed[7-9] that the isolated NAD(P)H coenzyme undergoes, in the presence of general acids $AH^{(+)}$, irreversible decomposition in its nicotinamide section[10,11] and, hence, deactivation. Studies[12-18] of reactions of the model compounds of *I* indicate that final products of the acid catalysis have structures of type *II* (X = OH, $OCOCH_3$, SO_3^-). Formation of the latter is explained[14-17] with presumption of a reversible protonation pre-equilibrium at C(5) position of *I* and subsequent irreversible attack of C(6) position by a nucleophile $X^{(-)}$ or XH. In the case of the complete coenzyme it is obvious[19-24] that the role of the XH nucleophile is played by 2'-hydroxyl group in the ribose fragment linked by a nucleoside bond to the dihydronicotinamide part of the NAD(P)H coenzyme molecule. The present communication deals with quantum-chemical study of probability of the protonation step in the mentioned transformations, the simple NADH model *I* (R = CH_3) being studied by the EHT, CNDO/2, MNDO and *ab initio* STO-3G methods.

* Part XVI in the Series On Calculations of Biologically Important Compounds; Part XV: This Journal *47*, 1621 (1982).

CALCULATIONS

The calculations were carried out by means of standard programs using an IBM 370/145, an ICL-4-72 and a CYBER 172 computers. The used parameters of the semi-empirical methods were the same as those in previous communications of this series. The parametrization of the MNDO method was identical with the originally published program[25], and in the case of the non-empirical calculation we used the standard STO-3G bases[26]. The dependences of E_{EHT} and $E_{CNDO/2}$ electron energies on distance parameters were calculated by 25 pm steps. The geometry of the *I* fragment was chosen in accordance with ref.[27,28]. The energy map of the system $H^{(+)}$–*I* ($R = CH_3$) was represented by means of square network of coordinates (600 pm side) where calculation of the EHT energies at the individual intersections gave 625 E_{EHT} values. The protonated forms *III*, *IV* and *V* were optimized by the gradient method[29] based on the CNDO/2 wave functions. The starting point for the MNDO optimization was the geometries *IIIa,b* and *IV* derived from structure *I* by modification of hybridization at the protonated centres C(5) and C(3), respectively. The geometries obtained by the MNDO optimization were used for the non-empirical calculation.

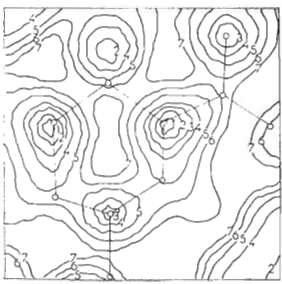

FIG. 1

Map of EHT energies for the system *I*–$H^{(+)}$. The $H^{(+)}$ particle moves in a plane parallel with that of the heterocycle *I* at a distance of 100 pm. Zero energy corresponds to the value −96 177·4 kJ mol^{-1}, the line **1** corresponds to an energy increase of 1 kJ mol^{-1} as compared with zero level, similarly line 2 (25 kJ mol^{-1}), 3 (50 kJ mol^{-1}), 4 (75 kJ mol^{-1}), 5 (125 kJ mol^{-1}), 6 (175 kJ mol^{-1}) and 7 (225 kJ mol^{-1})

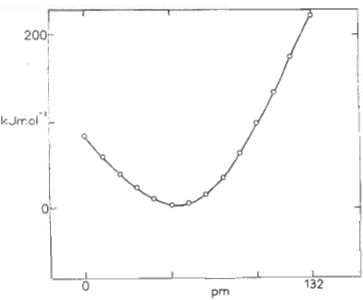

FIG. 2

Dependence of CNDO/2 energy on *b* parameter for the system *I*–$H^{(+)}$. The particle $H^{(+)}$ moves at a distance of 120 pm above C(5)—C(6) bond, and *b* denotes horizontal distance from C(5) centre

RESULTS AND DISCUSSION

Configuration of $H^{(+)}$–*I* (R = CH_3) *supermolecule.* At the EHT level we used (as in ref.[28]) the way of evaluation of the local energy minima (LEM) with the $H^{(+)}$ particle moving above the plane of *I* molecule at a 100 pm distance. The corresponding EHT map is given in Fig. 1. It clearly shows five LEM near the positions N(1), C(3), O(3c), C(5) and hydrogen atom at C(4). The deepest are three minima at C(3), C(5) and H—C(4), which indicates the protonation of the heterocyclic part of the molecule (perpendicular to the symmetry plane of the molecule) to be easier than protonation of oxygen atom O(3c) of amide group. Formation of cations *IV* and *III* is presumed to be the final result of the protonations at C(3) and C(5) positions. In this context, meaning of the third minimum for H—C(4) is not clear. It can represent a consequence of neglection of electronic repulsion between these hydrogen

TABLE I

Geometry of *IIIa* ion after finished CNDO/2 gradient optimization with respect to all degrees of freedom

A—B—C—D centres	A—B bond length, pm	A—B—C valence angle, °	A—B—C—D dihedral angle, °
N(1)—C(2)—C(3)	141·2	134·5[a]	123·7[b]
C(4)—C(3)—C(2)—N(1)	146·6	120·9	0·0
C(5)—C(4)—C(3)—C(2)	147·9	115·6	0·0
C(6)—C(5)—C(4)—C(3)	144·0	117·3	0·0
C(1)—N(1)—C(2)—C(3)	141·8	119·3	180·0
C(3a)—C(3)—C(2)—N(1)	145·7	116·7	180·0
N(3b)—C(3a)—C(3)—C(2)	136·9	119·6	180·0
O(3c)—C(3a)—C(3)—C(2)	127·8	121·3	0·0
H(2)—C(2)—N(1)—C(1)	111·7	112·7	0·0
H_a(4)—C(4)—C(3)—C(2)	112·6	108·6	123·9
H_b(4)—C(4)—C(3)—C(2)	112·6	108·6	−123·9
$H_a(3_b)$—N(3b)—C(3a)—C(3)	106·1	121·5	0·0
H_b(3b)—N(3b)—C(3a)—C(3)	106·2	123·4	180·0
H_a(5)—C(5)—C(4)—H_a(4)	112·8	112·8	— 1·5
H_b(5)—C(5)—C(4)—H_b(4)	112·8	112·8	1·5
H(6)—C(6)—C(5)—C(4)	111·9	118·9	180·0
H_a(1)—C(1)—N(1)—C(2)	111·9	110·8	−120·1
H_b(1)—C(1)—N(1)—C(2)	111·9	111·2	0·0
H_c(1)—C(1)—N(1)—C(2)	111·9	110·8	120·1

[a] C(2)—C(3) bond length, pm; [b] N(1)—C(2)—C(3) valence angle.

centres in the EHT method. Also the map in Fig. 1 shows that the minima at C(3) and C(5) do not lie strictly above the corresponding atomic centres, hence the optimum protonation coordinates are probably deviated from the directions precisely perpendicular to the heterocycle plane. In the case of the protonation at C(5) position, this presumption was supported by the CNDO/2 calculation, too, in which we followed the $E_{CNDO/2}$ energy changes during the proton shift along C(5)—C(6) bond 120 pm above the plane of *I* heterocycle. From Fig. 2 it follows that the proton shift by 55 pm towards the C(6) centre is most favourable energetically.

Molecular geometry of the protonated forms. With respect to the fact that the EHT method found two deepest energy minima above the C(3) and C(5) positions, we tried to compare energies of the corresponding cations *III* and *IV* at a semi-empirical level. For this purpose we carried out the CNDO/2 gradient optimization of geo-

TABLE II

Geometry of *IV* ion after finished CNDO/2 gradient optimization with respect to all degrees of freedom

A—B—C—D centres	A—B bond length, pm	A—B—C valence angle, °	A—B—C—D dihedral angle, °
N(1)—C(2)—C(3)	142·2	154·5[a]	120·0[b]
C(4)—C(3)—C(2)—N(1)	147·8	116·6	19·9
C(5)—C(4)—C(3)—C(2)	145·3	116·0	— 2·8
C(6)—N(1)—C(2)—C(3)	142·5	116·6	— 18·1
C(1)—N(1)—C(2)—C(3)	144·1	114·7	63·3
C(3a)—C(3)—C(2)—N(1)	144·1	65·5	142·6
N(3b)—C(3a)—C(3)—C(2)	137·2	131·1	119·0
O(3c)—C(3a)—C(3)—C(2)	135·9	105·6	— 36·5
H(2)—C(2)—C(3)—C(4)	113·1	116·8	152·8
H(3)—C(3)—C(2)—N(1)	112·4	118·9	—117·8
H_a(3b)—N(3b)—C(3a)—O(3c)	106·8	112·6	—153·7
H_b(3b)—N(3b)—C(3a)—O(3c)	106·8	113·3	— 28·2
H_a(4)—C(4)—C(3)—C(2)	112·8	108·2	122·7
H_b(4)—C(4)—C(3)—C(2)	112·9	106·9	—127·1
H(5)—C(5)—C(4)—C(3)	111·3	117·4	172·3
H(6)—C(6)—C(5)—C(4)	112·3	119·7	171·7
H_a(1)—C(1)—N(1)—C(6)	114·7	119·9	— 15·9
H_b(1)—C(1)—N(1)—C(6)	112·1	113·1	109·8
H_c(1)—C(1)—N(1)—C(6)	112·6	107·4	—131·5

[a] C(2)—C(3) bond length, pm; [b] N(1)—C(2)—C(3) valence angle.

metry of the models *IIIa,b* and *IV*. The CNDO/2 gradient optimization[29] of the *IIIa,b* and *IV* structures started from a geometry with plane ring conformation derived from structure *I* by modification of hybridization at the protonated centres C(5) and C(3), respectively; the carbamoyl group was considered planar. Tables I and II summarize the CNDO/2-optimized geometries of the C(5)- and C(3)-protonated forms. In the case of the C(5)-protonated geometry *III*, it gives the geometry *IIIa* whose energy (with respect to that of *IIIb*) decreased by 46 kJ mol^{-1} after the CNDO/2 gradient optimization. Table I reveals that the optimization of the C(5)--protonated form *IIIa* resulted in a structure with maintained nearly coplanar conformation of the ring and amide group and, hence, their mutual conjugation. This result corresponds to sp^2 hybridization at N(1) atom (maximum conjugation of free electron pair at nitrogen with the other π electrons). From Fig. 3 it follows that in the optimized form *IIIa* a considerable (+0·23) positive CNDO/2 charge obtained for C(6) position in accordance with the probable subsequent attack of this position by the nucleophile X to give the product *II* (R = = CH_3). Compared with the given optimization results of the C(5)-protonated form *IIIa*, the optimization of the C(3)-protonated form *IV* gave unexpected results. In this case the protonation should cause interruption of conjugation between the electron system of double bonds and the amide group, but, in addition to it, the optimized form *IV* shows a dramatic change of the configuration type at the N(1) centre which rather corresponded to sp^3 hybridization (Table II). This result is

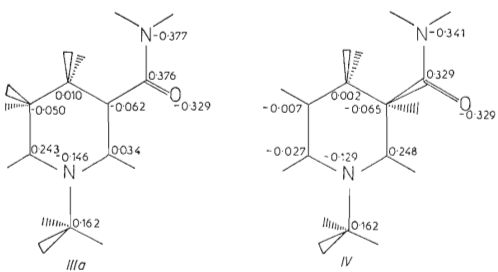

FIG. 3

Electron distribution in *IIIa* and *IV* ions after finished MNDO optimization. The values are given in e.

TABLE III

Geometry of *IIIa* and *IIIb* ions after finished MNDO optimization with respect to all degrees of freedom

A—B—C—D centres	*IIIa*			*IIIb*		
	A—B bond length, pm	A—B—C valence angle, °	A—B—C—D dihedral angle, °	A—B bond length, pm	A—B—C valence angle, °	A—B—C—D dihedral angle, °
N(1)—C(6)—C(5)	132·6	150·5[a]	122·6[b]	144·4	150·6[a]	123·6[b]
C(4)—C(5)—C(6)—N(1)	154·5	116·9	— 0·3	154·1	116·1	— 1·7
C(3)—C(4)—C(5)—C(6)	151·5	115·4	0·2	150·9	115·0	1·7
C(2)—C(3)—C(4)—C(5)	136·5	120·8	0·2	135·7	122·6	— 0·8
C(1)—N(1)—C(2)—C(3)	150·6	118·2	—179·6	150·4	118·6	—178·9
C(3a)—C(3)—C(2)—N(1)	151·9	118·0	—178·9	151·7	119·8	176·7
N(3b)—C(3a)—C(3)—C(2)	138·6	120·6	—177·6	140·5	116·4	80·2
O(3c)—C(3a)—C(3)—C(2)	123·3	121·3	4·4	122·5	121·8	— 93·6
H(2)—C(2)—N(1)—C(6)	109·7	113·1	—179·6	109·5	114·5	179·8
H_a(4)—C(4)—C(3)—C(2)	111·5	109·3	—121·6	111·5	109·1	—123·2
H_b(4)—C(4)—C(3)—C(2)	111·5	109·3	121·6	111·6	109·0	121·6
H_a(5)—C(5)—C(4) —C(3)	111·7	110·0	121·9	111·7	110·0	123·7
H_b(5)—C(5)—C(4)—C(3)	111·7	109·9	—121·8	111·7	109·9	—120·3
H(6)—C(6)—N(1)—C(1)	110·4	119·8	— 0·1	110·2	119·5	— 0·2
$H_a(3_b)$—N(3b)—C(3a)—C(3)	99·9	120·2	172·0	100·5	116·5	171·5
$H_b(3_b)$—N(3b)—C(2a)—C(3)	99·1	123·2	12·7	100·1	116·8	37·6
H_a(1)—C(1)—N(1)—C(2)	111·2	109·0	119·9	111·2	109·0	118·0
H_b(1)—C(1)—N(1)—C(2)	110·9	110·6	0·0	110·9	110·5	— 1·0
H_c(1)—C(1)—N(1)—C(2)	111·2	108·6	—119·5	111·2	108·9	—120·8

[a] C(6)—C(5) bond length, pm; [b] N(1)—C(6)—C(5) valence angle.

interpreted as a calculation artefact of the gradient optimization[29] of the *IV* ion with respect to all degrees of freedom on the basis of its CNDO/2 wave function. Also striking in this connection is the little realistic preference of the thus optimized ion *IV* to the isomeric ion *IIIa* by as much as 696·4 kJ mol^{-1}. However, possible interaction of the proton with amide group of *I* must not be neglected, either. Therefore, the gradient optimization was also carried out for the ion structures *Va – d*, but the planar conformations showed no distinct changes. Their CNDO/2 molecular energies are somewhat preferred to those of the C(5)-protonated form *IIIa* (in kJ mol^{-1}): 94·6 (*Va*), 83·3 (*Vb*), 89·6 (*Vc*) and 90·5 (*Vd*). It must not, however, be forgotten that formation of these species will be not very likely in enzyme catalysis due to hydrogen bonds of amide group in coenzyme *I* and suitable amino groups of apoenzyme. In aqueous media, however, the O-protonated forms *Va – d* will undoubtedly form equilibrium mixtures with the C-protonated forms *III* and *IV* and,

TABLE IV

Geometry of *IV* ion after finished MNDO optimization with respect to all degrees of freedom

A—B—C—D centres	A—B bond length, pm	A—B—C valence angle, °	A—B—C—D dihedral angle, °
N(1)—C(2)—C(3)	132·8	152·4[a]	124·7[b]
C(4)—C(3)—C(2)—N(1)	155·1	113·6	2·9
C(5)—C(4)—C(3)—C(2)	150·0	115·9	— 2·4
C(6)—C(5)—C(4)—C(3)	135·3	124·3	0·5
C(1)—N(1)—C(6)—C(5)	150·5	117·4	179·3
C(3a)—C(3)—C(2)—N(1)	155·6	109·3	— 122·7
N(3b)—C(3a)—C(3)—C(2)	139·1	117·1	— 151·9
O(3c)—C(3a)—C(3)—C(2)	122·9	121·6	33·7
H(2)—C(2)—N(1)—C(1)	110·3	119·1	— 2·2
H(3)—C(3)—C(2)—N(1)	112·0	104·6	120·7
H_a(4)—C(4)—C(5)—C(6)	111·6	107·7	125·4
H_b(4)—C(4)—C(5)—C(6)	111·7	108·0	— 121·3
H(6)—C(6)—N(1)—C(1)	109·2	115·6	0·5
H_a(3b)—N(3b)—C(3a)—C(3)	100·3	118·1	172·9
H_b(3b)—B(3b)—C(3a)—C(3)	99·9	119·6	29·3
H_a(1)—C(1)—N(1)—C(6)	111·2	108·5	— 87·6
H_b(1)—C(1)—N(1)—C(6)	111·1	110·1	151·9
H_c(1)—C(1)—N(1)—C(6)	111·1	109·6	32·5

[a] C(2)—C(3) bond length, pm; [b] N(1)—C(2)—C(3) valence angle.

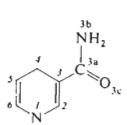

I

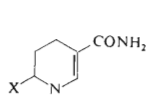

II

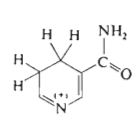

IIIa

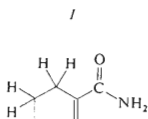

IIIb

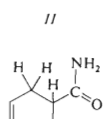

IV

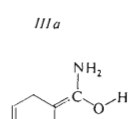

Va

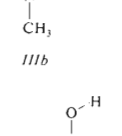

Vb

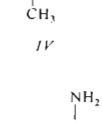

Vc

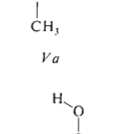

Vd

moreover, occurrence of the individual protonations will be strongly affected by solvent effects which were not involved explicitely in our considerations. To verify our presumption about non-adequacy of the CNDO/2 molecular geometry of *IV* ion, we repeated the geometry optimization of the two isomeric ions using, this time, the basis of MNDO wave functions[25]. The results are given in Tables III and V. The calculation for the C(3)-protonated form *IV* indicates a realistic almost planar arrangement of the heterocycle, *i.e.* it shows the expected discrepancy to the artefact result of the CNDO/2 procedure. In contrast to this fact, introduction of the MNDO optimization for the C(5)-protonated form *IIIa,b* does not result in any substantial geometry change as compared with that obtained for the heterocycle by the CNDO/2 gradient procedure; depending on choice of the starting orientation of amide group it gives the optimized geometriss of two *Z*- and *E*-conformers *IIIa,b*. It is only noteworthy that the conformers *IIIa* and *IIIb* differ distinctly in their torsion angle of amide group at C(3)—C(3a) bond (Table IV), the amide group being practically coplanar with and practically perpendicular to the plane of the heterocycle in the

ion *IIIa* and *IIIb*, respectively. Table VI compares the calculated energy characteristics for the ions *III* and *IV* inclusive of the non-empirical STO-3G energies. Obviously, the MNDO optimization leads to preference of the C(5)-protonated form *IIIb* on the basis of both the total energies (by almost 19 kJ mol^{-1}) and the heats of formation. The *ab initio* MO calculation using the STO-3G bases prefers then the both C(5)-protonated forms *IIIa,b*, even though less distinctly than the semi-empirical MNDO method does.

TABLE V

Total and relative energies and heats of formation of the systems studied

Molecule	MNDO			STO-3G	
	E_{tot} [a]	E_{rel} [b]	E_{form} [b]	E_{tot} [a]	E_{rel} [b]
IIIa	−65·4084	23·07	661·32	−449·364534617	2·06
IIIb	−65·4172	0·00	638·23	−449·365318446	0·00
IV	−65·4101	18·71	645·96	−449·364477904	2·21

[a] Non-dimensional units defined as $X = E/h$, where $h = 2\,628{\cdot}1$ kJ mol^{-1}; [b] kJ mol^{-1}.

TABLE VI

Charge population of the ions studied

Centre	MNDO			STO-3G		
	IIIa	*IIIb*	*IV*	*IIIa*	*IIIb*	*IV*
N(1)	−0·146	−0·144	−0·129	−0·175	−0·173	−0·171
C(2)	0·034	0·023	0·248	0·037	0·029	0·207
C(3)	−0·062	−0·064	−0·065	0·035	0·038	−0·057
C(4)	0·010	0·009	0·002	−0·104	−0·103	−0·104
C(5)	−0·050	−0·047	−0·007	−0·109	−0·109	−0·002
C(6)	0·243	0·244	−0·027	0·204	0·204	0·025
C(N1)	0·162	0·162	0·162	−0·061	−0·061	−0·060
C(3a)	0·376	0·344	0·329	0·306	0·302	0·308
N(3b)	−0·377	−0·332	−0·341	−0·441	−0·427	−0·431
O(3c)	−0·329	−0·282	−0·329	−0·238	−0·222	−0·250

Electron populations in ions III *and* IV. The calculated atomic charges and expansion coefficients of the LUMO frontier orbitals are given in Tables VII and VIII. Obviously, the MNDO and STO-3G data lead to similar conclusions concerning subsequent attack of a nucleophilic reagent on the substrates *III* and *IV*. In the MNDO and STO-3G energy-preferred C(5)-protonated form *IIIb*, the C(6) position is the site of both the highest positive charge and the greatest expansion coefficient in the LUMO, which fully agrees with the experimentally derived[14-17] structure of the final adducts *II*. The same criteria, however, should indicate that, for the C(3)-protonated form *IV*, 2 position is preferently attacked by nucleophile, which would cause the structure of the adducts formed to differ distinctly from the case *II*.

Thus the shown MO calculations indicate that protonation of nicotinamide fragment in NADH (representing a catalytic initial step followed by nucleophilic addition to dihydropyridine nucleus) leads to formation of the ions *III* – *V* (including the C(5)-protonated forms *IIIa,b*)which could generate the experimentally found[14-17] type of addition products *II* in a subsequent nucleophilic attack. Both electronic and orbital structure of the *IIIa,b* ions is favourable for the attack of C(6) position by nucleophile $X^{(-)}$ which obviously represents a decisive discrimination step for the tranformation $I + HX \rightarrow II$.

TABLE VII

MNDO and STO-3G expansion coefficient of the LUMO of the ions studied. Numerically are given the values $|c_i| \geq 0{\cdot}1$ only

Centre	MNDO			STO-3G		
	IIIa	*IIIb*	*IV*	*IIIa*	*IIIb*	*IV*
N(1)	−0·437	0·447	−0·465	0·499	0·529	−0·542
C(2)	−0·160	0·135	0·775	0·203	0·159	0·825
C(3)	0·359	−0·352	+	−0·406	−0·394	+
C(4)	−	+	−	−	−	−
C(5)	−	+	0·345	+	+	0·388
C(6)	0·768	−0·776	−0·101	−0·805	−0·825	−0·146
C(N1)	−	+	−	+	+	−
C(3a)	+	−	+	−	−	0·113
N(3b)	−	−	+	+	−	+
O(3c)	−	−	−	0·177	−	−

REFERENCES

1. Van Eikeren P., Greirer D. L.: J. Amer. Chem. Soc. *98*, 4655 (1976).
2. Shinkai S., Kunitake T.: Chem. Lett. *1977*, 297.
3. Shinkai S., Hamada H., Manabe O.: Tetrahedron Lett. 1397, *1979*.
4. Shinkai S., Nakano T., Hamada H., Kusano Y., Manabe O.: Chem. Lett. 16, *1979*, 229.
5. Adams M. J., Buehner M., Chandrasekhar K., Ford G. C., Hackert M. L., Liljas A., Rossmann M. G., Smiley I. E., Allison W. S., Everse J., Kaplan N. O., Taylor S. S.: Proc. Nat. Acad. Sci. U.S.A. *70*, 1968 (1973).
6. Moras D., Olsen K. W., Sabesan M. N., Buehner M., Ford G. C., Rossmann M. D.: J. Biol. Chem. *250*, 9137 (1975).
7. Warburg O., Christian W.: Biochem. Z. *274*, 112 (1934).
8. Von Euler H., Schlenk F., Heinwinkel H., Hegberg B.: Z. Physiol. Chem. *256*, 208 (1936).
9. Haas E.: Biochem Z. *288*, 123 (1936).
10. Karrer P., Kahnt F. W., Epstein R., Jaffe W., Ishii T.: Helv. Chim. Acta *21*, 233 (1938).
11. Karrer P., Stare F. J.: Helv. Chim. Acta *20*, 418 (1937).
12. Wallenfels K., Schüly H.: Biochem. Z. *329*, 75 (1957).
13. Anderson A. G., Berkelhammer G.: J. Amer. Chem. Soc. *80*, 992 (1958).
14. Stock A., Sann E., Pfleiderer G.: Justus Liebigs Ann. Chem. *647*, 188 (1961).
15. Diekmann H., Englert G., Wallenfels K.: Tetrahedron *20*, 281 (1964).
16. Kim C. S. Y., Chaykin S.: Biochemistry *7*, 2339 (1968).
17. Hope H.: Acta Crystallogr., Sect. B *25*, 78 (1969).
18. Choi K. S., Alivisatos S. G. A.: Biochemistry *7*, 190 (1968).
19. Oppenheimer N. J.: Biochem. Biophys. Res. Commun. *50*, 683 (1973).
20. Oppenheimer N. J., Kaplan N. O.: Biochemistry *13*, 4673 (1974).
21. Williams T. J., Ellis P. D., Brysch T. A., Fisher R. R., Dunlap R. B.: Arch. Biochem. Biophys. *176*, 275 (1976).
22. Miles D. W., Urry D. W., Eyring H.: Biochemistry *7*, 2333 (1968).
23. Johnson S. L., Tuazon P. T.: Biochemistry *16*, 1175 (1977).
24. Miksic J. R., Brown P. R.: Biochemistry *17*, 2234 (1978).
25. Dewar M. J. S., Thiel W.: J. Amer. Chem. Soc. *99*, 4899, 4907 (1977).
26. Hehre W. J., Steward J. S., Pople J. A.: J. Chem. Phys. *51*, 2657 (1969).
27. Kuthan J., Musil L.: This Journal *42*, 859 (1977).
28. Kuthan J., Böhm S., Skála V.: This Journal *44*, 99 (1979).
29. Pancíř J.: Theor. Chim. Acta *29*, 21 (1973).

Translated by J. Panchartek.